Microwave Photonic Mixer Based on Polarization Rotation and Polarization-Dependent Modulation

Qi Zhou and Mable P. Fok, *Member, IEEE*

***Abstract*— A microwave photonic mixer capable of both amplitude and phase modulation is proposed and experimentally demonstrated. This scheme utilizes single-sideband modulation in dual-drive Mach–Zehnder modulator and polarization rotation in semiconductor optical amplifier to generate a pair of phase coherent optical carriers with different polarizations, while a polarization sensitive Mach–Zehnder intensity modulator (MZM) is used for modulating the IF signal onto one of the generated carrier. Both the optical and the electrical spectra are measured and show successful frequency mixing. By setting the bias point of the MZM at slightly different voltages, our scheme supports binary-phase-shift keying, on–off keying, and amplitude-shift keying modulations. Widely opened eye diagrams and clear waveforms are experimentally obtained for all modulations. Moreover, the proposed scheme does not have a hard limit on the supported lowest local oscillator frequency and no reconfiguration is needed when a frequency change in the local oscillator is required.**

***Index Terms*— Microwave photonics, frequency modulation, mixers.**

I. Introduction

THE rapidly growing demands on high-speed any-time any-where multimedia services have driven the need of a significant increase in data-rates in wireless communication network [1]. Due to the broadband, high-capacity, and low-loss characteristics of fiber optics, radio-over-fiber (RoF) techniques are the most efficient way to distribute and transmit high-speed multimedia signals. To meet the growing demand of high data-rate wireless communications as well as to fully utilize the capacity of optical fiber, microwave photonic signal processing techniques have attracted lots of research interests [2]. In RoF, the microwave signal is first modulated onto a high-frequency carrier (usually refers as the local oscillator (LO)) with an electrical mixer, and then this modulated signal is used to modulate the optical carrier for transmitting in the optical fiber. Due to the increasing data-rate demanded by the high-speed wireless system as well as the corresponding high-frequency carrier needed, the frequency requirement reaches the bandwidth limitation of electrical mixer. With the broadband and low loss characteristic of photonics, photonics based microwave mixer can realize ultra-wideband mixing operation and can support RF signal and LO that are at distributed locations. Due to the high isolation provided by photonic components, the microwave photonic mixer has an infinite isolation between RF, IF, and LO ports [3] which is a desired feature in most microwave systems. Various approaches for demonstrating a microwave photonic mixer has been proposed, including the use of cascading Mach-Zehnder modulators (MZM) [4], a dual-parallel MZM [5], dual-wavelength phase modulation followed by optical filtering [6], single-wavelength phase modulation with stimulated Brillouin scattering for carrier suppression [3], as well as single sub-carrier modulation together with LO mixing from a separate optical path [7]–[10]. However, the existing approaches are either having low conversion efficiency, suffering from the disability for phase modulation, or requiring complicated off-line digital signal processing for compensating the phase incoherence between carriers. Recently, a photonic microwave mixing technique based on coherent orthogonal optical carriers' generation has been demonstrated [11], which solves the challenges mentioned above. However, spectral filtering is required during coherent orthogonal carriers generation which hinder the ability to tune the LO frequency as well as setting a limit to the lowest possible frequency for the LO.

In this letter, we present and experimentally demonstrate a microwave photonic mixer that works well for both amplitude and phase modulation without the need of complicated off-line processing for phase compensation or an optical filter that limits the LO frequency range. The elimination of an optical filter removes the lower frequency limit imposed on the LO as well as enables flexible tuning of LO frequency. The ability to tune the LO frequency can potentially enable dynamic spectral access and enhance transmission security. Principle of the proposed optical mixer is based on the use of single-sideband modulation in a dual-drive MZM followed by polarization rotation in a semiconductor optical amplifier (SOA) for the generation of phase coherent optical carriers. Both the power of the single-sideband signal and the SOA bias current are optimized, such that when a single-sideband signal is launched into the SOA, the phase shift is the same for both the transverse-electric (TE) and transverse-magnetic (TM) modes of the carrier, however, the $+1^{st}$ order sideband will have a different phase shift between its TE and TM mode [12]. Thus, polarization angle discrepancy between the optical carrier and the $+1^{st}$ order sideband is resulted and a pair of phase coherent carriers with different polarization are obtained. The proposed scheme can support a

Manuscript received May 27, 2015; revised July 22, 2015; accepted August 16, 2015. Date of publication August 19, 2015; date of current version October 2, 2015. This work was supported in part by the National Science Foundation through the Division of Computer and Network Systems under Grant 1217435 and in part by Princeton University under a subcontract.

The authors are with the Lightwave and Microwave Photonics Laboratory, College of Engineering, University of Georgia, Athens, GA 30602 USA (e-mail: qizhou1991722@gmail.com; mfok@uga.edu).

Color versions of one or more of the figures in this letter are available online at http://ieeexplore.ieee.org.

Digital Object Identifier 10.1109/LPT.2015.2470121

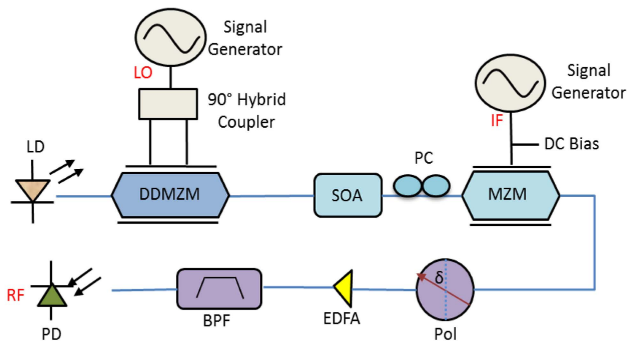

Fig. 1. Experimental setup of the microwave photonic mixer. LD: laser diode, DDMZM: dual-drive Mach-Zehnder modulator; SOA: semiconductor optical amplifier; PC: polarization controller; MZM: Mach-Zehnder intensity modulator; Pol: polarizer; EDFA: Er-doped fiber amplifier; BPF: bandpass filter; PD: photodetector; LO: local oscillator; IF: intermediate frequency, RF: radio frequency.

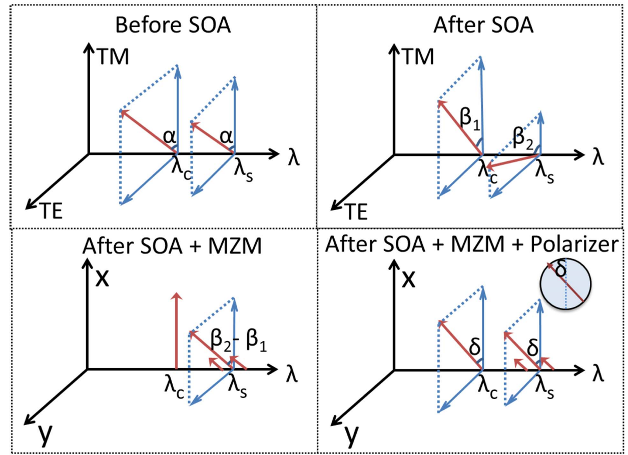

Fig. 2. Principle of the proposed microwave photonic mixer based on polarization rotation in SOA.

wide range of frequency [13] that is governed by the modulator bandwidth, which significantly extends the lower frequency range of the LO (as low as 1 GHz) as well as improves the frequency tunability of the LO. Furthermore, the phase coherent optical carriers are generated in one single path, such that phase fluctuation between the carriers can be avoided. In this letter, we are demonstrating up-conversion where a LO is mixing with an intermediate frequency (IF) signal such that a radio frequency (RF) signal is resulted. The MZM for modulating the IF signal onto the optical carrier is polarization sensitive, such that TE and TM axis of the MZM have different modulation efficiencies. As a result, the IF signal will mainly be modulated onto the $+1^{\text{st}}$ order sideband by aligning it to the high modulation efficiency axis in the MZM. Due to the phase coherence of the optical carrier and $+1^{\text{st}}$ order sideband, our approach supports both amplitude modulation and phase modulation. With the proposed scheme, we have successfully demonstrated the modulation of phase stable binary-phase-shift keying (BPSK), amplitude-shift keying (ASK) and on-off keying (OOK) signals. Widely opened eye diagrams and clear waveforms are obtained for all of the modulation formats.

II. Experimental Setup

Fig.1 shows the experimental setup of the proposed microwave photonic mixer for up-conversion. A distributed feedback (DFB) laser at λ_c is used as the light source for modulation in the dual-drive Mach-Zehnder modulator (DDMZM). Sinusoidal microwave signal f_{LO} is used as the LO, which is launched to the DDMZM via a 90° hybrid coupler. By properly setting the bias voltage applied to the DDMZM, single-sideband modulation with more than 30-dB suppression on the -1^{st} order sideband is obtained. The optical fields of the carrier and $+1^{\text{st}}$ order sideband are governed by

$$\begin{pmatrix} \boldsymbol{E_c(t)} \\ \boldsymbol{E_s(t)} \end{pmatrix} = \begin{bmatrix} E_c \cdot e^{j(\omega_c t+\varphi_0)} \\ E_s \cdot e^{j\omega_s t} \end{bmatrix} \tag{1}$$

$\boldsymbol{E_c(t)}$ and $\boldsymbol{E_s(t)}$ are the optical fields of the carrier and the $+1^{\text{st}}$ order sideband respectively, while E_c and E_s are the corresponding amplitudes of the optical fields. ω_c, ω_s and φ_0 are the optical frequencies of the carrier and $+1^{\text{st}}$ order sideband, and the initial phase difference between them, respectively. Fig. 2 illustrates polarization evolution of the carrier and the $+1^{\text{st}}$ sideband in SOA as well as during IF modulation process in MZM. TE and TM are the axis of the SOA, and the output of the DDMZM at 5 dBm is launched to the SOA at a polarization angle of α with respect to the TM axis of SOA. Phase shift induced onto the carrier is the same for both TE and TM modes, while the phase shift induced onto the $+1^{\text{st}}$ order sideband are different for the TE and TM mode [12].

Thus, there is a polarization rotation in the $+1^{\text{st}}$ order sideband relative to the polarization of the carrier, resulting in new polarization angles of β_1 and β_2 for the carrier and $+1^{\text{st}}$ order sideband with respect to the TM axis of the SOA, respectively. Ideally, polarization between the carrier and the $+1^{\text{st}}$ order sideband should be orthogonal to obtain the best modulation performance by the IF. The MZM for IF modulation also consists of both TE and TM axis, we refer the two axis as x and y. Then, we align the output signal of SOA to the MZM axis such that the carrier is aligned with the x axis. Thus, output from the SOA can be expressed as:

$$\begin{pmatrix} \boldsymbol{E_{out\text{-}c}(t)} \\ \boldsymbol{E_{out\text{-}s}(t)} \end{pmatrix} = \begin{bmatrix} E_{c-x} \cdot e^{j(\omega_c t+\varphi_0)} \\ E_{s-x} \cdot e^{j\omega_s t} + E_{s-y} \cdot e^{j\omega_s t} \end{bmatrix} \tag{2}$$

here, $\boldsymbol{E_{out\text{-}c}(t)}$ and $\boldsymbol{E_{out\text{-}s}(t)}$ are the output fields of the SOA at optical frequency ω_c and ω_s. E_{c-x}, $E_{s-x}$and E_{s-y} represent the field amplitudes of the carrier and sideband at polarization axis x and y, respectively. Output signal of the SOA, which is a pair of phase coherent carriers is aligned to the MZM axis such that the carrier polarization is aligned with the x-axis that has minimum modulation efficiency, while the $+1^{\text{st}}$ order sideband polarization is aligned close to the y-axis such that it experiences a significantly efficient modulation. IF signal at f_{IF} is applied to the MZM and the optical field can be written as

$$\begin{pmatrix} \boldsymbol{E'_{out\text{-}c}(t)} \\ \boldsymbol{E'_{out\text{-}s}(t)} \end{pmatrix} = \begin{bmatrix} E_{c-x} \cdot e^{j(\omega_c t+\varphi_0)} \\ E_{s-x} \cdot e^{j\omega_s t} + E'_{s-y}(t) \cdot e^{j(\omega_s t+\partial(t))} \end{bmatrix} \tag{3}$$

where $\boldsymbol{E'_{out\text{-}c}(t)}$ and $\boldsymbol{E'_{out\text{-}s}(t)}$ represent the fields of the carrier and $+1^{\text{st}}$ order sideband at the output of the MZM.

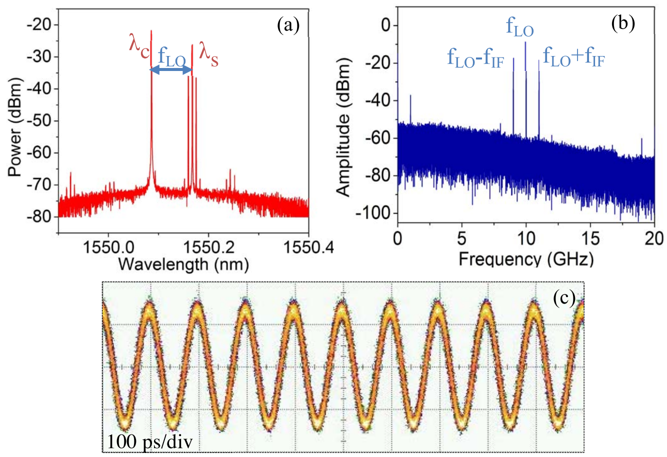

Fig. 3. (a) Optical spectrum measured after the polarizer. (b) Electrical spectrum of the PD output. (c) Waveform of the LO with the frequency at 10 GHz.

$E'_{s-y}(t)$ and ∂(t) are the intensity and phase modulation on the $+1^{st}$ order sideband, respectively. A polarizer is placed after the MZM and has its polarization angle (δ) aligned in between the two polarization states of the carrier and $+1^{st}$ order sideband, such that the polarization component at δ is extracted from both the carrier and $+1^{st}$ order sideband for beating at the photodetector (PD). The optical process is completed at this point and the resultant signal at polarization δ can be expressed as:

$$\boldsymbol{E_\delta(t)} = E_{c-\delta}\cdot e^{j(\omega_c t+\varphi_0)} + E_{x-\delta}\cdot e^{j\omega_s t} + E_{y-\delta}(t)\cdot e^{j[\omega_s t+\partial(t)]} \tag{4}$$

where δ is the polarization angle of the polarizer with respect to the x axis and $\boldsymbol{E_\delta(t)}$ represents the output field of the polarizer. δ is optimized such that the eye diagram at the optical mixer output has the best performance. $E_{c-\delta}$, $E_{x-\delta}$, $E_{y-\delta}(t)$ are the amplitudes of the δ polarization component of the carrier and $+1^{st}$ order sideband along the x- and y-axis. The measured optical spectrum after the polarizer is depicted in Fig. 3(a), which shows that the IF signal is only modulated onto the $+1^{st}$ order sideband (indicated by the sub-sideband around λ_s) but not the carrier. An Er-doped fiber amplifier is used to provide amplification while a 0.4nm band-pass filter is used to suppress the amplified-spontaneous-emission noise. A 10-GHz photodetector is used to convert the optical signal back to electrical domain. According to the square law detection, the photocurrent is governed by:

$$\begin{aligned} I_{PD} \sim \boldsymbol{E_\delta}(t)\cdot\boldsymbol{E^*_\delta}(\mathrm{t}) = {} & \underbrace{E^2_{c-\delta} + E^2_{x-\delta}}_{\text{DC Component}} \\ & + \underbrace{2\cdot E_{c-\delta}\cdot E_{y-\delta}(t)\cdot\cos\left[2\pi f_{LO}t+\varphi_0-\partial(t)\right]}_{\text{Mixing Signal}} \\ & + \underbrace{2\cdot E_{c-\delta}\cdot E_{x-\delta}\cdot\cos\left[2\pi f_{LO}t+\varphi_0\right]}_{\text{LO}} \\ & + \underbrace{2\cdot E_{x-\delta}\cdot E_{y-\delta}(t)\cdot\cos[\partial(t)] + E^2_{y-\delta}(t)}_{\text{BasebandSignal}} \end{aligned} \tag{5}$$

where $\boldsymbol{E^*_\delta}$(t) is the conjugate of $\boldsymbol{E_\delta(t)}$ and f_{LO} is the newly generated microwave signal, which equals to the optical frequency difference between the carrier and the $+1^{st}$ order sideband. As shown in equation (5), the mixing signal indicated as $2\cdot E_{c-\delta}\cdot E_{y-\delta}(t)\cdot cos[2\pi f_{LO}t+\phi_0-\partial(t)]$ has been produced. With the PD, the intensity and phase that were modulated on the $+1^{st}$ order sideband at the MZM are now converted to the intensity and phase modulation of the generated electrical carrier f_{LO}. Electrical spectrum of the PD output is shown in Fig. 3(b). New frequency components at f_{LO}, $f_{LO}-f_{IF}$ and $f_{LO}+f_{IF}$ have been generated, indicate that frequency mixing and signal modulation are achieved. Fig. 3(c) is the PD output measured by a 40-GHz oscilloscope when no IF signal is being applied to the MZM. A clear sinusoidal waveform with stable amplitude has been generated, which indicates that the phase coherence between the optical carrier and the $+1^{st}$ order sideband has been maintained throughout the whole system.

III. Results and Discussion

OOK modulation and ASK modulation are the fundamental modulation schemes in RoF systems due to its simplicity in implementation and demodulation. To investigate the performance of the proposed microwave photonic mixer, we first study the modulation of ASK and OOK signal onto a 10-GHz microwave carrier. A 10-GHz sinusoid microwave signal is generated from a signal generator and is used to drive the DDMZM as a LO. A 1-Gbps $2^{15}-1$ pseudo-random-bit-sequence (PRBS) signal is used as the IF signal, which is used to drive the polarization sensitive MZM. Polarization of the input light is set such that the carrier is aligned with the MZM axis with minimum modulation efficiency, such that the PRBS signal is modulated onto the $+1^{st}$ order sideband but not the carrier. The MZM is biased at the positive slope of the transmission curve, where bit-0 voltage level is aligned with the minimum transmission point of the MZM. Thus, an OOK modulation is obtained on the 10 GHz LO after being detected by the PD. Widely-opened eye diagrams of the modulated signal are resulted and are shown in Fig. 4(a)-4(b). Fig. 4(a) is the eye diagram showing four complete bits in the PRBS signal, while Fig. 4(b) is the zoom-in view within one bit. When an eight-bit bit sequence of 11010010 is applied to the MZM as an IF signal, a clear waveform is shown in Fig. 4(c) while a zoom-in view is shown in Fig. 4(d). Both Fig. 4(c)-4(d) clearly indicate OOK modulation of the 10-GHz LO is successfully achieved and a conversion efficiency of 3-dB is obtained, which is comparable to existing approaches. To achieve ASK modulation, the MZM for IF modulation is biased at a point on the positive slope such that bit-0 voltage level is aligned slightly away from the minimum transmission point of the MZM. Both a PRBS signal and a 11010010 sequence are used as the IF signals. Widely opened eye diagrams and clear waveforms are obtained as shown in Fig. 4(e) – 4(h), indicating ASK modulation of the LO is achieved.

Phase modulation capability is crucial to enable advanced modulation schemes for improved transmission capacity and performance. The carrier and the $+1^{st}$ order sideband generated in our scheme have good phase coherence between them; thus, our scheme also works well for phase modulation

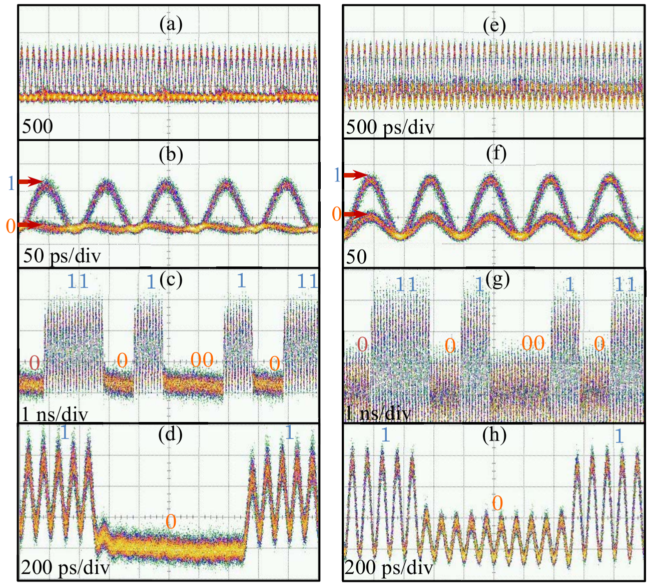

Fig. 4. (a)-(b) Eye diagrams of PRBS OOK modulation at 1-Gbps; (c)-(d) 11010010 bit sequence OOK modulation; (e)-(f) Eye diagrams of PRBS ASK modulation at 1-Gbps; (g)-(h) 11010010 bit sequence ASK modulation.

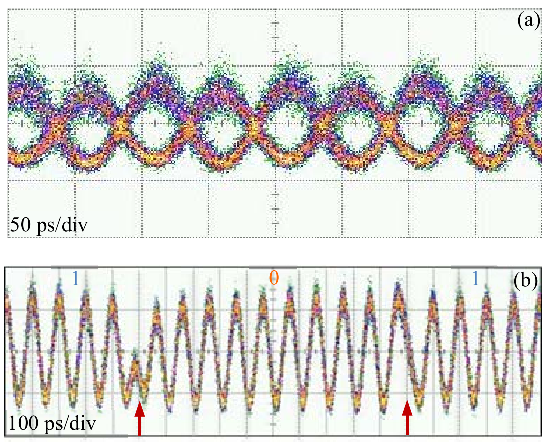

Fig. 5. 1-Gbps phase modulation (a) Eye diagram; (b) Waveform.

without the need of complex off-line signal processing for phase compensation. To perform phase modulation, the MZM for IF modulation is biased at its minimum transmission point such that a 0 phase is resulted when the modulating signal is a bit 0, while π phase is resulted when the signal is a bit 1. A 1-Gbps $2^{15}-1$ PRBS signal is used as the IF for modulation. Fig. 5(a) is a zoom-in view of the resulting eye diagram after phase modulation, which clearly indicates the 0 phase and π phase of the BPSK signal. The eye diagram is noisier than the amplitude modulated counterpart due to the insufficient nonlinear polarization rotation in the SOA for the generation of orthogonal optical carriers. A bit sequence with alternative 1 and 0 is used as the IF signal to observe the change in phase. Fig. 5(b) is the waveform with the edges of the bits marked by the red arrows. During bit 0, the valley of the 10-GHz LO is aligned with the vertical grid lines, representing 0 phase; while the peak of the 10-GHz LO is aligned with the vertical grid line during bit 1, which indicates a π phase shift in the LO.

IV. Conclusion

In summary, we propose and demonstrate photonic mixer scheme that is capable for performing both amplitude and phase modulation. Our approach utilizes SSB generation in DDMZM and polarization rotation in SOA for the generation of phase coherent optical carriers. Various modulation schemes including OOK, ASK and BPSK have been implemented and verified by the resultant widely opened eye diagrams and clear waveforms. Our scheme does not have a hard limit on the supported lowest LO frequency and the LO frequency can be tunable without the need of reconfiguring the setup.

References

[1] Z. Jia, J. Yu, G. Ellinas, and G.-K. Chang, "Key enabling technologies for optical–wireless networks: Optical millimeter-wave generation, wavelength reuse, and architecture," *J. Lightw. Technol.*, vol. 25, no. 11, pp. 3452–3471, Nov. 2007.

[2] J. Yao, "Microwave Photonics," *J. Lightw. Technol.*, vol. 27, no. 3, pp. 314–335, Feb. 1, 2009.

[3] E. H. W. Chan and R. A. Minasian, "High conversion efficiency microwave photonic mixer based on stimulated Brillouin scattering carrier suppression technique," *Opt. Lett.*, vol. 38, no. 24, pp. 5292–5295, Dec. 2013.

[4] G. K. Gopalakrishnan, W. K. Burns, and C. H. Bulmer, "Microwave-optical mixing in $LiNbO_3$ modulators," *IEEE Trans. Microw. Theory Techn.*, vol. 41, no. 12, pp. 2383–2391, Dec. 1993.

[5] Y. Gao *et al.*, "An efficient photonic mixer with frequency doubling based on a dual-parallel MZM," *Opt. Commun.*, vol. 321, pp. 11–15, Jun. 2014.

[6] B. M. Haas and T. E. Murphy, "Linearized downconverting microwave photonic link using dual-wavelength phase modulation and optical filtering," *IEEE Photon. J.*, vol. 3, no. 1, pp. 1–12, Feb. 2011.

[7] T. Nagatsuma *et al.*, "Terahertz wireless communications based on photonics technologies," *Opt. Exp.*, vol. 21, no. 20, pp. 23736–23747, Oct. 2013.

[8] M. Zhu, L. Zhang, S.-H. Fan, C. Su, G. Gu, and G.-K. Chang, "Efficient delivery of integrated wired and wireless services in UDWDM-RoF-PON coherent access network," *IEEE Photon. Technol. Lett.*, vol. 23, no. 13, pp. 1127–1129, Jul. 1, 2012.

[9] X. Li, Z. Dong, J. Yu, N. Chi, Y. Shao, and G. K. Chang, "Fiber-wireless transmission system of 108 Gb/s data over 80 km fiber and 2×2 multiple-input multiple-output wireless links at 100 GHz W-band frequency," *Opt. Lett.*, vol. 37, no. 24, pp. 5106–5108, Dec. 2012.

[10] S. Koenig *et al.*, "Wireless sub-THz communication system with high data rate," *Nature Photon.*, vol. 7, no. 12, pp. 977–981, Sep. 2013.

[11] J. Zheng *et al.*, "Photonic microwave-signal-mixing technique using phase-coherent orthogonal optical carriers for radio-over-fiber application," *Opt. Lett.*, vol. 39, no. 18, pp. 5263–5266, Sep. 2014.

[12] H. Jiang *et al.*, "Improved optical single-sideband generation using the self-modulation birefringence difference in semiconductor optical amplifiers," *Opt. Lett.*, vol. 32, no. 17, pp. 2580–2582, Sep. 2007.

[13] J. Ge, H. Feng, G. Scott, and M. P. Fok, "High-speed tunable microwave photonic notch filter based on phase modulator incorporated Lyot filter," *Opt. Lett.*, vol. 40, no. 1, pp. 48–51, Jan. 2015.